Molecular Nanotube Aggregates of β- and γ-Cyclodextrins Linked by Diphenylhexatrienes

Guang Li and Linda B. McGown*

Linked by strings of diphenylhexatriene (DPH) molecules, β- and γ-cyclodextrins (CDs) can form nanotube aggregates that contain as many as ~20 βCDs (20 nanometers long) or ~20 to 35 γCDs (20 to 35 nanometers long). Nanotube formation was indicated in solution, by fluorescence anisotropy and light scattering results, and on graphite surfaces, by scanning tunneling microscopy. Tubes were not observed for the smaller αCDs. Molecular modeling shows that CD cavity size and the rodlike DPH structure are key factors in nanotube formation. Spectra generated by proton nuclear magnetic resonance indicate the inclusion of DPH in the interior of the CDs and formation of nanotubes in βCDs and γCDs only. The photophysical properties of DPH are affected by its arrangement into a one-dimensional array within the CD nanotube, possibly because of exciton formation.

Cyclodextrins (CDs) are cyclic polysaccharide compounds in which six (αCD), seven (βCD), or eight (γCD) glucose monomers are linked to form a truncated conical structure. CDs have found diverse uses in both fundamental and applied research (*1*). Recently, it was reported that αCD can be threaded onto a polymer chain of polyrotaxanes (*2*) or poly(iminooligomethylene)s (*3*) to form a "molecular necklace" that can then be converted into a molecular nanotube by the covalent cross-linking of adjacent αCD units on the polymer chain (*4*). The molecular necklaces and nanotubes contain ~20 and ~15 αCDs, respectively (*2*, *4*). These structures have generated much interest as alternatives to the carbon nanotube (*5*), reflecting growing interest in the design of supermolecular assemblies to serve as molecular devices.

We report the formation of rigid molecular nanotube aggregates of βCD and γCD through linkage by the rodlike molecules of *all-trans*-1,6-diphenyl-1,3,5-hexatriene (DPH). This formation of nanotubes was shown by dynamic fluorescence anisotropy (DFA), scattered light intensity measurements, and scanning tunneling microscopy (STM) (*6*) and supported by fluorescence, ultraviolet (UV) absorption, and ^{1}H nuclear magnetic resonance (NMR) spectroscopic measurements. Molecular modeling provides a physical explanation and a possible structure for the nanotubes.

Internal rotation of a fluorophore and the overall rotation of a fluorophore-host complex can be studied by DFA (*7*, *8*). DPH is a good probe of fluorescence anisotropy because it exhibits isotropic behavior (*7*). The DFA measurements of DPH in the CDs showed a major component (preexponential factor $\alpha > 0.85$ in βCD and > 0.90 in γCD) with a rotational correlation time $\phi > 200$ ns in βCD and > 500 ns in γCD. The steady-state anisotropy, $\langle r \rangle$, of DPH was 0.321 ± 0.004 in βCD and 0.353 ± 0.002 in γCD. These values are close to the limiting anisotropy of DPH [$r_0 = 0.38$ at the excitation wavelength (λ_{ex}) = 325 nm] (*9*), which indicates little reorientation of DPH during the lifetime of its excited state. Thus, DPH appears to be included in the βCD or γCD cavity and involved in the formation of very large aggregates.

In contrast, DFA measurements of DPH in αCD yielded a major component with a short rotational correlation time [$\phi = 0.79$ ± 0.01 ns at temperature (T) = 20.0°C and $\phi = 0.45$ ± 0.01 ns at T = 40.0°C]. The correlation times follow Debye-Stokes-Einstein behavior and, assuming a spherical complex, indicate a hydrodynamic radius of 9.0 Å (*8*), which is in the range of the spherical hydrodynamic radii of the αCD monomer and dimer (8.0 and 9.7 Å, respectively). Thus, the stoichiometry of DPH to αCD is on the order of 1:1 or 1:2. The steady-state anisotropy of DPH in αCD was 0.066 ± 0.007, which is significantly smaller than for DPH in βCD or γCD.

The scattered light intensities were calculated as the differences between the intensities for CD solutions in the presence of DPH (0.176 ± 0.007 for αCD, 1.748 ± 0.007 for βCD, and 1.78 ± 0.01 for γCD) and the intensities for the corresponding CD solutions without DPH (0.129 ± 0.005 for αCD, 0.589 ± 0.001 for βCD, and 0.305 ± 0.001 for γCD). The differences increase from 0.047 ± 0.007 for DPH in αCD to 1.158 ± 0.007 for DPH in βCD and 1.47 ± 0.01 for DPH in γCD. This result indicates the formation of large aggregates in the solutions of DPH in βCD and γCD but not in αCD.

An explanation for the formation of long, rodlike complexes is provided by molecular modeling. Up to two DPH molecules can be included in βCD and up to three can fit into the γCD cavity, whereas only one DPH molecule can be included in αCD (Fig. 1A). In addition to the size of the CD cavity, the rigid, rodlike structure of DPH is a key factor in the formation of the nanotube aggregates. In the βCD or γCD cavities, the DPH molecules are partially overlapped with one another, like layers of bricks in a wall (Fig. 1B), and their motions are restricted. In the molecular mechanics calculations, stringing DPH molecules through the CDs in this manner lowers the total energy of the system. Defects in the tubelike aggregates (Fig. 1C) may occur, causing higher total energies and possibly breaking an aggregate or terminating its growth, which could serve to

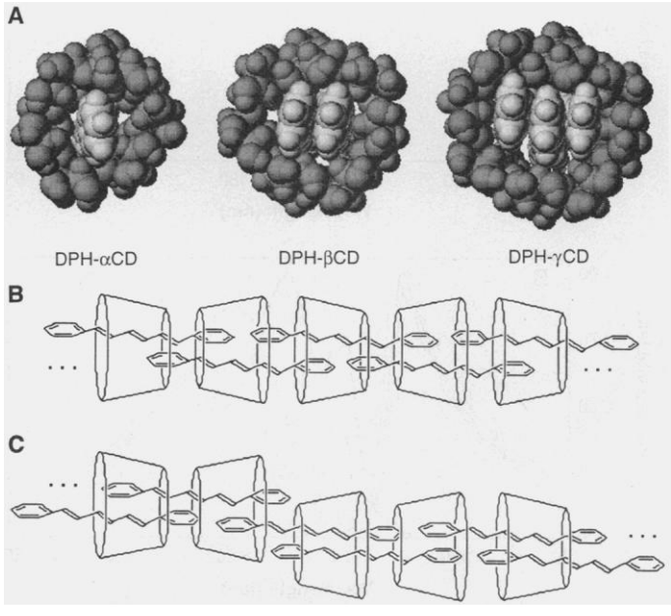

Fig. 1. Models for the DPH-CD nanotubes. (**A**) Molecular models of DPHs inside αCD, βCD, and γCD viewed along the long axis. (**B**) The linear nanotube aggregate of βCD. (**C**) Possible defect of βCD aggregates.

Department of Chemistry, P. M. Gross Chemical Laboratory, Duke University, Box 90346, Durham, NC 27708, USA.

*To whom correspondence should be addressed.

limit the length of the nanotubes.

Because the molecular modeling calculations did not include solvent molecules, they cannot be used to calculate equilibrium aggregate sizes. The rotational correlation times obtained from the DFA, however, indicate that the rigid nanotube aggregates could contain at least 20 βCDs (~20 nm long) or 30 γCDs (~30 nm long). The rodlike aggregates of DPH-βCD and DPH-γCD on graphite surfaces were imaged by STM. The average length and width of six different DPH-βCD nanotubes, three of which are shown in Fig. 2, are 22 ± 1 nm and 2.0 ± 0.2 nm, respectively. This length is consistent with the value obtained from the rotational correlation time. The width of 2 nm is a little larger than an estimated value of 1.53 nm for the βCD molecule in the absence of water (*1*), possibly because of the effects of hydration (*10*). Five DPH-γCD tubes were observed, ranging in length from 20 to 35 nm. This result is also consistent with the length that was calculated from the rotational correlation time. Rodlike images were not observed for the DPH-αCD samples.

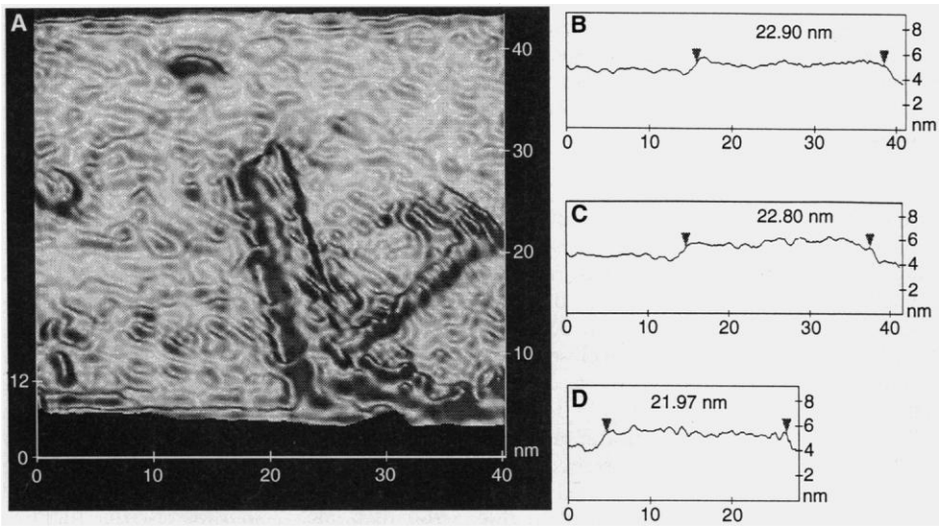

Fig. 2. DPH-βCD nanotube aggregates imaged by STM. One drop of the solution was deposited on a highly ordered pyrolytic graphite (HOPG) substrate and dried at least 2 hours. A NanoScope II scanning tunneling microscope (Digital Instruments) with head type A and a Pt-Ir wire tip was used in the constant height mode with a set point of 0.25 nA and a bias of 197.75 mV. The image was filtered to remove some noise. (**A**) Three DPH-βCD nanotubes, two together and one individual (rods 1, 2, and 3, from left to right). (**B** through **D**) The cross sections along rods 1, 2, and 3, respectivelv, and their length. The other images may be free CD molecules or clusters.

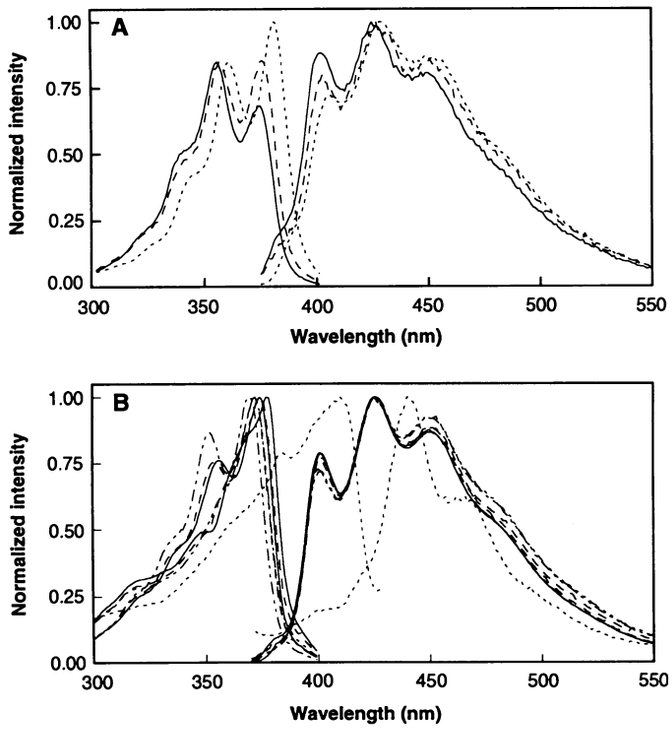

Fig. 3. The normalized excitation spectra [emission wavelength (λ_{em}) = 428 nm] and emission spectra (λ_{ex} = 325 nm) of (**A**) 15 μM DPH in aqueous CD solutions [αCD (solid line), βCD (dashed line), and γCD (dotted line)] and (**B**) 5 μM and 15 μM DPH in simple organic solvents (*12*): cyclohexane (solid lines), ethanol (dashed lines), methanol (dashed-dotted lines), and 15 μM DPH in water (dotted line). The intensity of DPH is about two orders of magnitude greater in the other solvents than in water, and its excitation spectrum was monitored at its maximum peak (λ_{em} = 440 nm) at very high gain; the bump at 384 nm is the Raman scattering peak of water.

The spectral peaks of DPH in the fluorescence excitation and emission spectra (Fig. 3) and UV absorption spectra are red-shifted in the order γCD > βCD relative to αCD, indicating an increasingly apolar microenvironment of DPH because the same trend is observed in simple organic solvents (Fig. 3B) (*11*). In addition, the peaks (absorption, excitation, and emission) on the red edge of the spectra are relatively enhanced relative to those on the blue edge, in the order γCD > βCD > αCD. Again, the same trend is observed in simple organic solvents; the peak on the blue side totally disappears in the excitation spectra when the concentration of DPH increases from 5 μM to 15 μM (*12*).

The spectral data indicate photophysical interactions between closely associated DPH molecules in both the larger CDs and the organic solvents at a DPH concentration of 15 μM. The effects in βCD and γCD are probably caused by partial overlap of DPH molecules within the CD nanotubes. In water, DPH is very insoluble, so its intensity is much lower than in the other solvents or the aqueous CD solutions. The spectral features of DPH in water are also different from those of any of the other solutions and may arise from the formation of DPH microcrystalline aggregates, which has been described for polycyclic aromatic hydrocarbons (*13*).

The observed red shift in the absorption and fluorescence spectra of DPH in βCD and γCD may also indicate exciton formation (*14*), which further supports the nanotube model in which DPHs are arranged like a one-dimensional "crystal" inside the threaded CD interiors. The photophysics of DPH and similarly rodlike, conjugated fluorescent molecules in CD nanotubes warrant further investigation.

The existence of nanotube formation in βCD and γCD solutions, but not in αCD solutions, in the presence of DPH is supported by ^{1}H NMR spectra (*15, 16*). In all CD solutions, two pairs of peaks, each separated by ~0.3 ppm, were observed in the DPH spectra in the chemical shift (δ) region of 6.2 to 8.4 parts per million (ppm). The pair at a higher value of δ was assigned to the aromatic protons, and the other pair was assigned to the conjugate protons. These DPH peaks shift upfield in the βCD and γCD solutions relative to αCD, and this shift appears to be greater for the aromatic protons than for the conjugate protons. This result indicates overlap of

DPH molecules in βCD and γCD, which is consistent with their inclusion within a CD nanotube, further supported by the difference between the DPH-CD spectra and the spectra of DPH alone in deuterated water (D_2O) and in chloroform ($CDCl_3$), which show different spectral features that are in the range of values for δ of ~6.5 to 7.5 ppm.

Our results suggest that DPH molecules provide a means for the linking of βCD or γCD into rodlike aggregates, or nanotubes, containing about 20 βCDs or 30 γCDs per tube on average. This is shown not only in the formation of the rigid nanotubes and their imaging by STM, but also in the achievement of an isolated, one-dimensional array of conjugated fluorescent molecules that may have the potential to function as a "molecular wire" or a photo switch at a supermolecular level through exciton formation or other processes (*17*).

REFERENCES AND NOTES

1. M. L. Bender and M. Komiyama, *Cyclodextrin Chemistry* (Springer-Verlag, New York, 1978); W. Seanger, *Angew. Chem. Int. Ed. Engl.* **19**, 334 (1980); J. Szejtli, *Cyclodextrins and Their Inclusion Complexes* (Akademiai Kiado, Budapest, 1982); J. Szejtli, *Cyclodextrin Technology* (Kluwer Academic, Dordrecht, 1988); S. Li and W. C. Purdy, *Chem. Rev.* **92**, 1457 (1992).
2. A. Harada, J. Li, M. Kamachi, *Nature* **356**, 325 (1992).
3. G. Wenz and B. Keller, *Angew. Chem. Int. Ed. Engl.* **31**, 197 (1992).
4. A. Harada, J. Li, M. Kamachi, *Nature* **364**, 516 (1993).
5. S. Iijima, *ibid.* **354**, 56 (1991).
6. Aqueous solutions of DPH (15 μM) in CDs (10 mM) were sonicated for 2 hours and then allowed to stand overnight. In the fluorescence measurements, excitation at 325 nm was provided by a He-Cd laser. The emission was selected at 400 to 560 nm with a combination of long-pass and short-pass filters (for the fluorescence lifetime and dynamic anisotropy measurements) and at 420 nm with a monochromator (for the steady-state anisotropy measurements). Scattered light intensity was measured 90° relative to the incident beam at 500 nm for both incident and scattered beams to avoid any absorption by the solutions. The temperature of the samples was kept at 20.0°C. In the STM experiments, two types of instruments (Digital and Burleigh) and tips (Pt-Ir and W) were used to image the nanotube aggregates on highly ordered pyrolytic graphite (HOPG).
7. A. Szabo, *J. Chem. Phys.* **81**, 150 (1984); A. Kawski, *Crit. Rev. Anal. Chem.* **23**, 459 (1993).
8. G. Li and L. B. McGown, *J. Phys. Chem.* **97**, 6745 (1993).
9. J. R. Lakowicz, H. Cherek, B. P. Mailiwal, *Biochemistry* **24**, 376 (1985).
10. P. K. Hansma, V. B. Elings, O. Marti, C. E. Bracker, *Science* **242**, 209 (1988); G. Lee, P. G. Arscott, V. A. Bloomfield, D. F. Evans, *ibid.* **244**, 475 (1989); P. G. Arscott, G. Lee, V. A. Bloomfield, D. F. Evans, *Nature* **339**, 484 (1989).
11. E. D. Cehelnik, R. B. Cundall, J. R. Lockwood, T. F. Palmer, *J. Phys. Chem.* **79**, 1369 (1975).
12. In all three organic solvents, the major peaks in the excitation spectra are red-shifted at the higher DPH concentration (15 μM) relative to the lower concentration (5 μM), and the peak at ~350 nm decreases in intensity. The emission spectra remain similar at the different DPH concentrations.
13. A. Nakajima, *Photochem. Photobiol.* **25**, 593 (1977); R. Weinberger and L. J. Cline Love, *Spectrochim. Acta* **40A**, 49 (1984); G. Li and L. B. McGown, unpublished results.
14. J. B. Birks, *Photophysics of Aromatic Molecules* (Wiley, New York, 1970), chap. 11; M. Orrit and P. Kottis, *Adv. Chem. Phys.* **74**, 1 (1988).
15. We obtained ^1H NMR (500 MHz) spectra with a Varian Unity 500 NMR Spectrometer in the Duke University NMR Spectroscopy Center. It was necessary to saturate the aqueous CD solutions with DPH (<1.0 mM) in order to obtain any signal. The solutions were centrifuged to remove precipitates and allowed to equilibrate overnight. The DPH concentration was too low in the solutions for observation of spectral fine structure. The spectra of the DPH-CD solutions were scanned from 19,000 to 30,000 times. The spectra of saturated DPH in D_2O and 1.0 mM DPH in $CDCl_3$ with no CD were also measured. The solution temperature was maintained at 20.0°C. The HOD water line was nulled by presaturation with a 1-s, low-power pulse from the transmitter to increase the dynamic range.
16. F. A. Bovey, L. Jelinski, P. A. Mirau, *Nuclear Magnetic Resonance Spectroscopy* (Academic Press, New York, ed. 2, 1988); E. Kolehmainen, *J. Colloid Interface Sci.* **127**, 301 (1989).
17. C. A. Mirkin and M. A. Ratner, *Annu. Rev. Phys. Chem.* **43**, 719 (1992).

18. We are grateful to L. A. Coury Jr. for helpful discussion of the STM results, to R. A. MacPhail for valuable comments, and to A. A. Ribeiro for assistance with the NMR experiments and interpretation. This work was supported by the Division of Chemical Sciences, Office of Basic Energy Sciences, Office of Energy Research, U.S. Department of Energy (grant DE-FG0588-ER13931), and by the Environmental Protection Agency (grant R817127-01).

19 November 1993; accepted 9 February 1994

Binding and Suppression of the Myc Transcriptional Activation Domain by p107

Wei Gu, Kishor Bhatia, Ian T. Magrath, Chi V. Dang, Riccardo Dalla-Favera*

An amino-terminal transactivation domain is required for Myc to function as a transcription factor controlling cell proliferation, differentiation, and apoptosis. A complementary DNA expression library was screened with a Myc fusion protein to identify proteins interacting with this domain, and a clone encoding the Rb-related p107 protein was isolated. The p107 protein was shown to associate with Myc in vivo and to suppress the activity of the Myc transactivation domain. However, mutant forms of Myc from Burkitt lymphoma cells, which contain sequence alterations in the transactivation domain, were resistant to p107-mediated suppression. Thus, disruption of a regulatory interaction between Myc and p107 may be important in tumorigenesis.

The *myc* proto-oncogene codes for a ubiquitously expressed nuclear phosphoprotein that functions as a transcriptional regulator controlling cell proliferation, differentiation, and apoptosis (*1*). Structural alterations of the *myc* locus, caused by chromosomal translocation, amplification, retroviral insertion, or retroviral transduction, are consistently associated with tumorigenesis in different species (*1*).

The expression of *myc* is tightly controlled at multiple levels, including transcription initiation and elongation and mRNA stability (*1*). Less is known about the mechanisms regulating Myc protein function. In vivo, Myc is found mainly in heterodimeric complexes with the related protein Max, and this interaction is mediated by helix-loop-helix (HLH) and leucine zipper (LZ) domains present at the COOH-terminus of both proteins (*2*). The Myc-Max complexes stimulate transcription (*3*) and cell proliferation (*4*), whereas Max-Max homodimers or heterodimers formed

W. Gu and R. Dalla-Favera, Division of Oncology, Department of Pathology, and Department of Genetics and Development, College of Physicians and Surgeons, Columbia University, New York, NY 10032, USA.
K. Bhatia and I. T. Magrath, Pediatric Oncology Branch, National Cancer Institute, Bethesda, MD 20892, USA.
C. V. Dang, Departments of Medicine and Cell Biology and Anatomy, and The Johns Hopkins Oncology Center, Johns Hopkins School of Medicine, Baltimore, MD 21205, USA.
*To whom correspondence should be addressed.

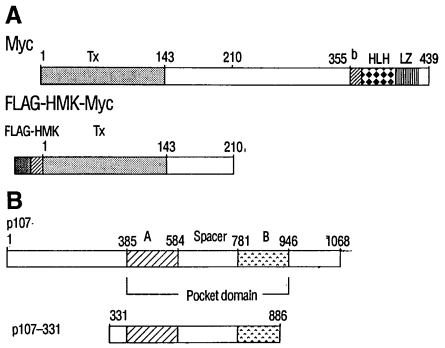

Fig. 1. Identification of proteins associated with the NH_2-terminal domain of Myc. (**A**) Schematic of normal Myc and the fusion protein (FLAG-HMK-Myc) used for screening the cDNA expression library. Tx, transcriptional activation domain. (**B**) Schematic of full-length p107 and of the protein (p107–331) predicted from the sequence of the positive cDNA clone. This clone codes for most of the pocket domain.